Desalination and Water Treatment
www.deswater.com

doi: 10.1080/19443994.2013.821041

52 (2014) 6333–6341
October

Taylor & Francis
Taylor & Francis Group

Numerical studies on the pressure-retarded osmosis (PRO) system with the spiral wound module for power generation

Sung-Soo Hong[a], Won Ryoo[a], Myung-Suk Chun[b], Seung Oh Lee[c], Gui-Yung Chung[a,*]

[a]*Department of Chemical Engineering, Hong-Ik University, Mapo-gu, Seoul 121-791, Korea*
Tel. +82 2 320 1681; email: gychung@hongik.ac.kr
[b]*Complex Fluids Laboratory, National Agenda Research Division, Korea Institute of Science and Technology (KIST), Seongbuk-gu, Seoul 136-791, Korea*
[c]*Department of Urban and Civil Engineering, Hong-Ik University, Mapo-gu, Seoul, 121-791, Korea*

Received 16 April 2013; Accepted 14 June 2013

ABSTRACT

The pressure-retarded osmosis system with the spiral wound module for power generation has been studied numerically. The system includes draw channel, membrane, and feed-channel. The water flux and the solute flux across membrane were calculated. In addition, changes in concentration, flow rate, and pressure of channel-fluids were obtained. Water flux across membrane decreases about 10% along the direction of draw-fluid in our system and increases slightly along the direction of feed-fluid. The concentration of draw-fluid decreases along the direction of draw-fluid. Power density is almost proportional to the inlet concentration difference, and increases at first and then decreases as the difference between inlet pressures of feed- and draw-fluids increases.

Keywords: Pressure-retarded osmosis (PRO); Spiral wound module; Membrane; Numerical modeling; Power density; Water flux

1. Introduction

The salinity gradient [1] is one of the renewable energy sources, which can be obtained from ocean, such as ocean waves, ocean currents, thermal gradient, and tides. Salinity gradient power systems use osmosis [2] and electrodialysis [3]. Here, the osmotically driven membrane process is operated in two types such as forward osmosis (FO) and pressure-retarded osmosis (PRO). The PRO system is studied in this research.

The PRO plant uses osmotic force to produce energy by mixing fresh water and sea water. When fresh water enters the membrane modules, part of fresh water is transferred by osmosis across membrane into sea water. Then, the pressurized sea water comes out as brackish water. This brackish water from the membrane module is split into two flows. About one-third of it goes to the turbine to generate power and two-thirds return to the pressure exchanger to pressurize the sea water of which typical operating pressure is 11–15 bars. Generating power through osmosis between river and sea water has been known since 1970s. Gerstandt et al. studied the membrane processes for an osmotic power plant and Statkraft in Norway started research on PRO in 1997 [4].

A significant portion of efforts to improve PRO conditions has been focused on tailoring the membrane structure to decrease the effects of internal

*Corresponding author.

concentration polarization (ICP) in the PRO system. So Phillip et al. [5] studied on a modeling describing the reverse permeation of draw solution across a membrane in FO operation and did experiments with NaCl. They measured the water permeability coefficient (A) and the salt permeability coefficient (B). These values were used in our modeling. Yip et al. [2] and Achilli et al. [6] have also studied water flux and solute flux through a flat membrane in considering concentration polarization which affects these fluxes for PRO. With the obtained water flux, they obtained power density. Similarly, Sundramoorthy et al. [7] carried out an analytical one-dimensional model for reverse osmosis (RO) spiral wound module.

In this study, the PRO spiral wound module has been studied. Compared with the previous works [6], two-dimensional modeling was studied in this work. Sea water and fresh water streams are introduced as cross-flows. Water and solute fluxes across membrane, pressure, salt concentration, flow rate, and power density for PRO system were obtained.

2. Model developments

2.1. System

The spiral wound module in Fig. 1(a) is the most common type used for reverse osmosis today. In the module, a combined layer of draw channel, membrane, and feed channel is wound around the central tube. Here, the membrane studied in this research was made of polyamide. The draw solution, i.e. sea water, in the draw channel flows in the axial direction of the module. On the other hand, fresh water in the feed channel flows in the circular direction around the central tube. While fresh water in the feed channel circulates around the central tube, part of it penetrates through the membrane in the radial direction of the module, mixes with the sea water, and flows in the draw channel along the axial direction of the module.

The unrolled configuration of spiral wound membrane is in Fig. 1(b). As mentioned above, one layer is composed of draw channel, membrane, and feed channel. Sea water flows in the x-direction through the draw channel and fresh water circulates in the y-direction around the central tube through the feed channel. Part of the fresh water penetrates through the membrane in the z-direction and flows axially with the sea water in the draw channel. The rest of the fresh water flows continuously and it is collected in the perforated central tube. Then, it flows in the axial direction of the tube and leaves the module [8]. Sea water in the draw channel gets pressure because

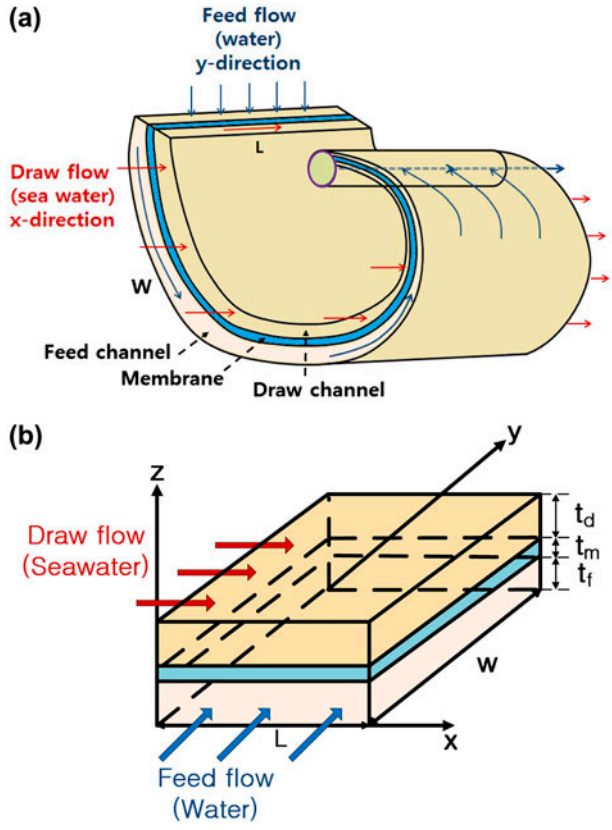

Fig. 1. The schematic diagram of the PRO system. (a) The spiral wound module and (b) the unrolled configuration of spiral wound membrane. Thicknesses of channels and membrane were expanded for visualization. Here, L is the length of cylindrical membrane and W is the width of the unfolded membrane. t_d, t_m, and t_f are the heights of draw-channel, membrane, and feed-channel, respectively.

of the fresh water which penetrates through the membrane. Power is obtained with the increased pressure.

2.2. Fluxes across the membrane

In the PRO system, the osmotic pressure is generated when a semi-permeable membrane separates two solutions of different concentrations. In this case, the osmotic pressure (π) can be calculated with the Van't Hoff equation [7,9]:

$$\pi = 2C_{\mathrm{NaCl}}RT \tag{1}$$

The theoretical osmotic pressure is 29 bar at 20°C for a 35 g/l salt solution, i.e. sea water.

The PRO system in Fig. 1(b) is composed of draw channel, membrane, and feed channel. Sea water flows in the x-direction through the draw channel and fresh water flows in the y-direction through the feed channel. In each channel, z-directional changes of pressure, concentration, and velocity were neglected.

They change only in x- and y-directions. In addition, diffusion was neglected compared with convection in channels.

In addition to the two cross-flows in two channels, there is a flow of solution in z-direction through pores in the membrane separating two channels as shown in Fig. 2. The solvent (i.e. water) and the solute (i.e. salt) move through the membrane due to the osmotic pressure and the concentration difference, respectively. The direction of water flux (J_w) is upward and it has a positive value. On the other hand, the direction of salt flux (J_s) is downward and it has a minus value. They are expressed as follows:

$$J_w = A\,(\Delta\pi_m - \Delta P_m) \tag{2}$$

$$J_s = -B\,(C_{d,m} - C_{f,m}) \tag{3}$$

Here subscripts d, f, and m stand for draw channel, feed channel, and membrane, respectively. A [m/(atm·s)] is the permeation coefficient of water and B [m/s] that of salt. ΔP_m is the local pressure difference across the membrane. To obtain more power, the membrane in the PRO process should have a high A-value and a low B-value. In addition, the inner structure of the membrane must not allow significant salt concentration to build up inside the membrane. Since the membrane is placed in a module, it must have a design that reduces the thickness of the support layer to a minimum without requiring too much energy for pumping water through the module [4].

McCutcheon et al. [10] modeled the water flux in the FO for improved membrane design. As shown in Fig. 2, the difference between the bulk concentrations of draw- and feed-channels ($C_{db}-C_{fb}$) includes the concentration difference across membrane ($C_{dm}-C_{fm}$). Here, we have to consider the concentration polarization influencing the performance of membrane separation processes. Concentration polarization due to an increased osmotic pressure at the membrane active layer surface is a significant problem in the membrane and it is detrimental to the water flux because it usually occurs on the surface of membrane. There are two concentration polarizations such as the ICP within the membrane and the external concentration polarization (ECP) on the outside surfaces of membrane. ECP can be significant for high-performance PRO membranes having low membrane structural parameters and high water fluxes [11]. Including these two concentration polarizations, Yip et al. [2] have obtained the water flux (J_w) as follows:

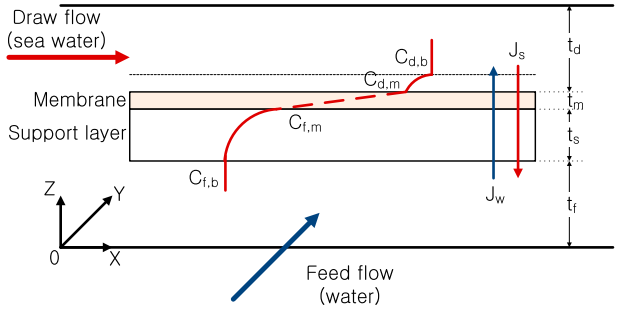

Fig. 2. The concentration distribution of salt across membrane. The water flux (J_w) has a positive value and the salt flux (J_s) has a minus one. Here, C_{fb} and C_{db} are bulk concentrations of feed- and draw-fluids, respectively. C_{fm} and C_{dm} are concentrations at membrane surfaces [2].

$$J_w = A\left[\frac{\pi_D \exp\left(-\frac{J_w}{k}\right) - \pi_F \exp\left(J_w\frac{S}{D}\right)}{1+\frac{B}{J_w}\left\{\exp\left(J_w\frac{S}{D}\right) - \exp\left(-\frac{J_w}{k}\right)\right\}} - \Delta P_m\right] \tag{4}$$

Here k [m/s] is the mass transfer coefficient for salt, S ($=t_s\tau/\varepsilon$) [m] the structural parameter of the support layer, and D [m^2/s] bulk diffusion coefficient. The ratio of S to D, i.e. (S/D), is called membrane resistivity (K). The value of membrane resistivity is given in Table 1. In obtaining the value of S, values of porosity and tortuosity of membrane were obtained from the reference [6] where similar membranes have been studied. The volumetric flow rates in the channels are affected by the membrane pore density (ε). Water penetrates from the feed channel to the draw channel through membrane pores. The larger the membrane pore density is, the more water flows through the membrane. As a result, the large power density would be obtained at a large membrane pore density. In a similar way, the flux of salt (i.e. solute) (J_s) was obtained as follows [2]:

$$\begin{aligned} J_s &= -B(C_{d,m} - C_{f,m}) \\ &= -B\left\{\frac{C_d \exp\left(-\frac{J_w}{k}\right) - C_f \exp\left(\frac{J_w S}{D}\right)}{1+\frac{B}{J_w}\left\{\exp\left(\frac{J_w S}{D}\right) - \exp\left(-\frac{J_w}{k}\right)\right\}}\right\} \end{aligned} \tag{5}$$

Table 1
Characteristic values of the PRO system [6,12]

Parameter	Value
Permeability coefficient of water, A [m/(atm s)]	9.5×10^{-7}
Permeability coefficient of salt, B [m/s]	8.5×10^{-8}
Structural parameter of the membrane, $S=t_s\tau/\varepsilon$ [m]	3.5×10^{-4}
Diffusion coefficient of salt, D [m^2/s]	1.5×10^{-9}
Membrane resistivity, $K(=S/D)$ [s/m]	2.3×10^{5}
Mass transfer coefficient of salt, k [m/s]	8.5×10^{-5}
Friction parameter in the feed- and the draw-channels, b [atm·s/m^4]	8,500

2.3. Balance equations

The total mass balance and the mass balance of salt in the draw and the feed channels are obtained including the above flux equations as follows [7]:

(1) In the draw channel:

$$\frac{du_d}{dx} = \frac{J_w}{t_d} \tag{6}$$

$$u_d \frac{dC_d}{dx} + C_d \frac{du_d}{dx} = \frac{J_s}{t_d} + \frac{J_w C_f}{t_d} \tag{7}$$

The increase of velocity due to the water flux (J_w in Eq. (4)) from the feed channel through membrane is shown in Eq. (6). The right-hand side of Eq. (7) includes the decrease of salt concentration due to the solute flux (J_s in Eq. (5)) and the increase of salt concentration due to the water flux (J_w) from the feed channel through membrane.

(2) In the feed channel:

$$\frac{du_f}{dy} = -\frac{J_w}{t_f} \tag{8}$$

$$u_f \frac{dC_f}{dy} + C_f \frac{du_f}{dy} = -\frac{J_s}{t_f} - \frac{J_w C_f}{t_f} \tag{9}$$

The decrease of velocity due to the water flux to the draw channel through membrane is shown in Eq. (8). The right-hand side of Eq. (9) includes the increase of salt concentration due to the solute flux (J_s) from the draw channel and the decrease of salt concentration due to the water flux (J_w) through membrane.

The volumetric flow rates (F_d and F_f) of draw- and feed-fluids are the multiplications of velocity (u) and cross-sectional area for each channel (i.e. ($w \cdot t_d$) and ($L \cdot t_f$)). Then, changes of volumetric flow rate are obtained with Eqs. (10) and (11) as follows:

$$\frac{dF_d}{dx} = wJ_w \tag{10}$$

$$\frac{dF_f}{dy} = -LJ_w \tag{11}$$

Changes of pressure in the channels are obtained with the volumetric flow rate following the Darcy's law [7]:

$$\frac{dP}{dy} = -bF \tag{12}$$

Here b (atm s m^{-4}) is the friction parameter whose value in the ref [12] was used in this modeling.

Membrane power density, W (W m^{-2}), can be calculated by multiplying the water flux (J_w) and the hydrostatic pressure difference across the membrane (ΔP) [2]:

$$W = J_w \Delta P \tag{13}$$

2.4. Calculations

The above equations were made dimensionless with the dimensionless parameters such as $X = x/L$. $Y = y/w$, $c_d = C_d/C_{do}$, and $c_f = C_f/C_{do}$. Here, C_{do} is the inlet salt concentration in the draw channel. Calculations were made in the finite difference method.

Parameter values used in the modeling are listed in Tables 1–3. Characteristic values of the system in Table 1 such as water permeability coefficient (A), solute permeability coefficient (B), and structural parameter of the membrane (S) were obtained from the references 6 and 12. Dimensions and parameter values of the system in Tables 2 and 3 were taken from the system in our laboratory. The inlet concentration of draw-fluid (sea water), is 35 g/l and that of feed-fluid (water) is 0 g/l. Reynolds numbers of the feed flow and the draw flow are in Table 3.

To observe effects of the difference between inlet concentrations of feed- and draw-fluids (ΔC_o), the inlet concentration of the feed-fluid is changed from the reference value of 0 g/l to 5, 10, and 20 g/l. The inlet pressure of the draw-fluid is 12 atm and that of the feed-fluid is 1 atm. The difference between the inlet pressures of feed and draw channels (ΔP_o) were observed by changing the inlet pressure of feed-fluid (P_{fo}) from the reference value of 1 atm to 7 and 12 atm.

The local water and salt fluxes (J_w and J_s) across membrane due to differences of concentration and

Table 2
Dimensions of the PRO system

Parameter	Value
Length of the module, L [m]	1
Width of the unrolled membrane, w [m]	8.4
Height of the feed channel, t_f [m]	8×10^{-4}
Height of the draw channel, t_d [m]	5×10^{-4}
Depth of the membrane, t_m [m]	4×10^{-5}

Table 3
Inlet parameter values used in the modeling

Channel	Parameter	Value
Feed	Concentration of salt, C_{fo} [g/l]	0, 10, 20
	Velocity of fluid, u_{fo} [m/s]	1.25
	Volumetric flow rate, F_{fo} [m^3/s]	1.0×10^{-3}
	Reynolds number	2,123
	Pressure, P_{fo} [atm]	1, 4, 8, 12
Draw	Concentration of salt, C_{do} [g/l]	35
	Velocity of fluid, u_{do} [m/s]	0.24
	Volumetric flow rate, F_{do} [m^3/s]	1.0×10^{-3}
	Reynolds number	593
	Pressure, P_{do} [atm]	12

pressure are obtained with Eqs. (4) and (5). Changes of flow rate and concentration in each channel are obtained with the mass balance equations including the water and the salt fluxes across membrane. Power density is calculated with local values of the water flux (J_w) and the pressure differences across membrane (ΔP) and averaged.

3. Results and discussion

Behaviors of the PRO system with the spiral wound module have been studied numerically. Water flux and solute flux across membrane were calculated. Furthermore, changes and distributions of pressure, concentration of salt, and velocities of channel-fluids were obtained. Power densities have been evaluated at various combinations of parameters.

3.1. The water flux across membrane

The driving forces for the water flux across membrane in the module are pressure difference and concentration difference across membrane. Hence, to observe effects of the pressure difference (i.e. ΔP_o, $(=P_{do}-P_{fo})$), the inlet pressure of draw channel (P_{do}) is fixed at 12 atm and the inlet pressure of feed channel (P_{fo}) is changed from 1 atm to 7 and 12 atm. So ΔP_o's become 11, 5, and 0 atm. Distributions of the water flux (J_w) across membrane at different inlet-pressure differences (ΔP_o) are shown in Fig. 3(a). As ΔP_o gets small, J_w becomes large. This can be explained with Eq. (2).

Effects of the inlet concentration difference (ΔC_o) on J_w are shown in Fig. 3(b). The inlet-concentration of the draw channel (C_{do}) is fixed at 35 g/l and the inlet-concentration of the feed channel (C_{fo}) is changed from 0 g/l to 10 and 20 g/l. So ΔC_o's become 35, 25, and 15 g/l. As ΔC_o gets small, J_w becomes small.

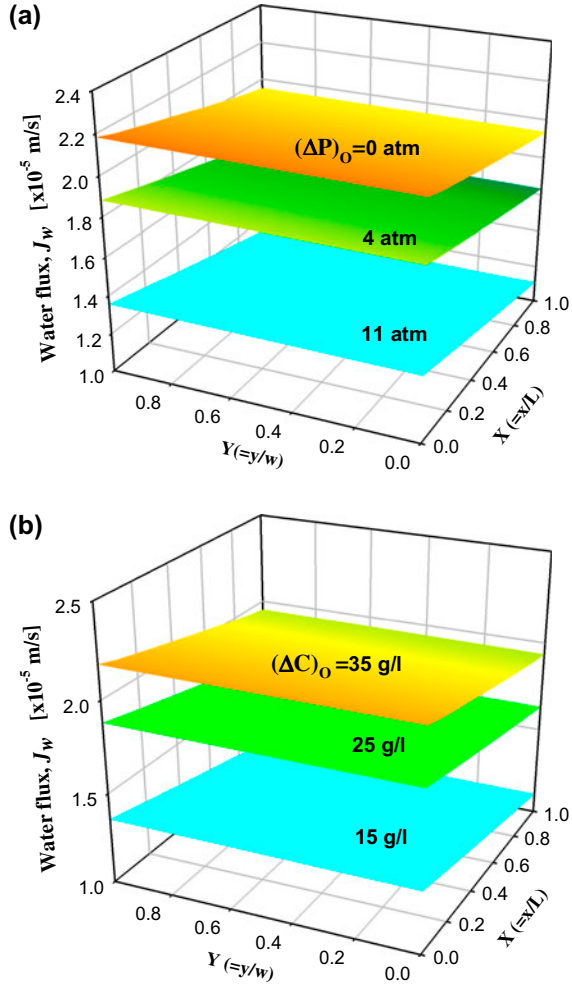

Fig. 3. Distributions of the water flux (J_w) across membrane at different (a) inlet-pressure differences (ΔP_o) and (b) inlet-concentration differences (ΔC_o) between feed- and draw-channels. Here, ΔP_o is $(P_{do}-P_{fo})$ and ΔC_o is $(C_{do}-C_{fo})$. P_{do} and C_{do} are fixed at 12 atm and 35 g/l, respectively.

This can also be explained with Eq. (2) as $\Delta\pi$ is proportional to ΔC.

The driving force for the solute (salt) flux (J_s) is the concentration difference. In addition, the driving force for the water flux (J_w) is the osmotic pressure which is proportional to the concentration difference. Hence, both J_w and J_s become big when the difference between the inlet concentrations of feed- and draw-fluids (ΔC_o) gets big. However, as mentioned above, the signs of J_w and J_s are different, i.e. J_w is a positive value and J_s is a minus value.

In both Figs. 3(a) and 3(b), J_w decreases about 10% along the direction of draw-fluid in our system and increases slightly along the direction of feed-fluid. The concentration of draw-fluid gets small because of the input of water from the feed-fluid. However, the

concentration of feed-fluid changes very small. So, ΔC gets small along the direction of flow and the osmotic pressure difference ($\Delta\pi$) also becomes small. As a result, J_w decreases along the direction of draw-fluid.

3.2. Changes of concentrations and flow rates of channel-fluids

As shown in Fig. 4(a), the concentration of draw-fluid decreases along the direction of draw-fluid because of the water flux (J_w) across membrane due to osmotic pressure. The concentration of draw-fluid at the exit becomes about 0.95 C_{do} in our system. About 5% of the concentration difference occurs while passing through the draw channel. The increase of the concentration of feed-fluid occurs due to the solute flux (J_s) from the draw-fluid across membrane. The change of feed concentration is very small compared with that of draw-fluid, such as $1/10^{-6}$ in size, as shown in Fig. 4(b). The concentration of feed-fluid (C_f) changes inversely, but in a similar way, as that of draw-fluid (C_d) does.

As in Eq. (2), there occurs a water-flow across membrane due to the osmotic pressure difference and the pressure difference. Because of this water-flow from the feed-fluid to the draw-fluid, the flow rate of feed-flow (F_f) decreases and that of draw-flow (F_d) increases as shown in Figs. 5 and 6.

Osmotic pressure is proportional to concentration as in Eq. (1). So, when the difference between the inlet concentrations of two channel fluids decreases, the water flux across membrane due to osmotic pressure difference decreases. As a result, changes of the flow rates in two channels appear similarly as those of concentration differences between two channels do. In other words, as the inlet-concentration difference

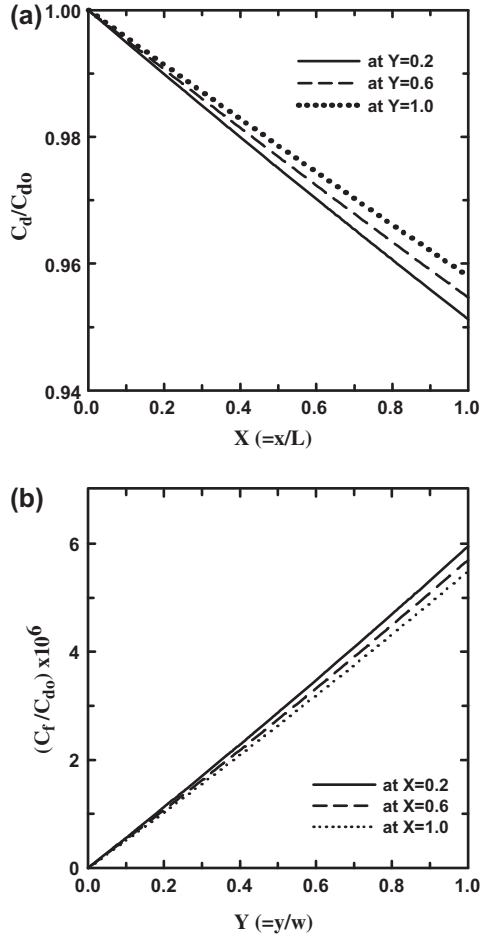

Fig. 4. Distributions of the dimensionless NaCl concentration (a) in the draw-channel (C_d/C_{do}) and (b) in the feed-channel (C_f/C_{do}) along the directions of flows. Here, C_{do}, P_{fo}, and ΔP_o are 35 g/l, 1, and 11 atm, respectively.

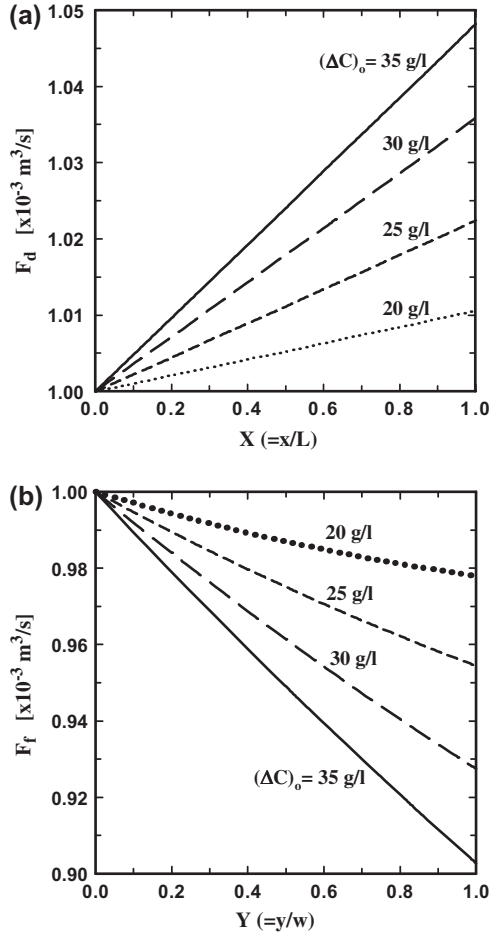

Fig. 5. Distributions of the volumetric flow rate (a) in the draw-channel and (b) in the feed-channel at different inlet NaCl concentration differences between draw- and feed-channels (ΔC_o). Here, ΔC_o is ($C_{do}-C_{fo}$). C_{do}, ΔP_o, and P_{fo} are 35 g/l, 11 and 1 atm, respectively.

(ΔC_o) becomes large, the flow rate in the draw-channel (F_d) increases as shown in Fig. 5(a) and that in the feed-channel (F_f) decreases as shown in Fig. 5 (b). The water flux decreases for the PRO system when the feed-fluid contains more salt [10].

Effects of the pressure difference between draw- and feed-fluids are opposite to those of the osmotic pressure difference. The pressure difference affects the water flux negatively as in Eq. (2). So, when the difference between the inlet pressures of two channel-fluids increases, the water flux across membrane due to pressure difference between two channel-fluids decreases. So, differently from the concentration difference, as the inlet-pressure difference between two channel fluids (ΔP_o) becomes large, the flow rate in the draw channel (F_d) decreases as shown in Fig. 6(a) and that in the feed channel (F_f) increases as shown in Fig. 6(b). This is because, as shown in Eq. (2), the driving force of the water flux from the feed to the draw channel is proportional to the value of ($\Delta\pi - \Delta P$), i.e. the osmotic pressure difference minus the pressure difference between two channels. So the driving force and, as a result, the water flux from the feed to the draw channel decrease with the increasing ΔP. So the increase of flow rate in the draw-channel and the decrease of flow rate in the feed-channel become small with the increasing ΔP.

3.3. The power density

A hydro-turbine extracts work from the expanding draw solution volume [13]. Part of the water from the draw-fluid goes to the turbine to generate power and the rest of the water returns to the pressure exchanger to pressurize sea water, i.e. draw-fluid. Hence, the pressure of draw-fluid is important.

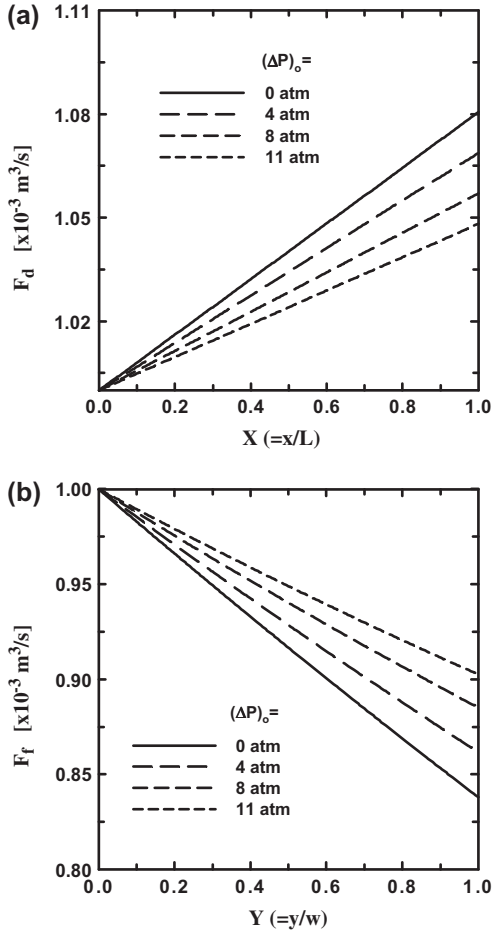

Fig. 6. Distributions of the volumetric flow rate (a) in the draw-channel and (b) in the feed-channel at different inlet pressure differences between draw- and feed- channels (ΔP_o). Here, ΔP_o is ($P_{do} - P_{fo}$). P_{do} is 12 atm and ΔC_o is 35 g/l.

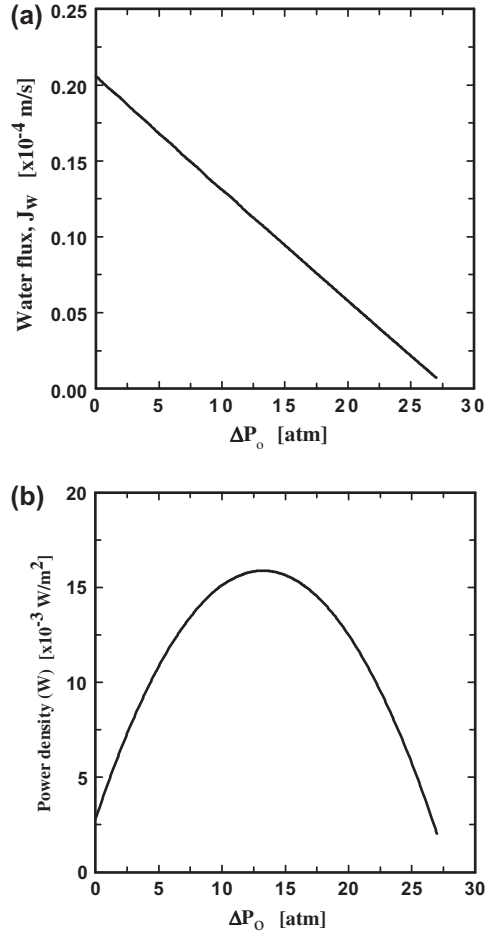

Fig. 7. Changes of (a) the average water flux (J_w) across membrane and (b) the power density with ΔP_o ($=P_{do} - P_{fo}$). Here, P_{fo} is fixed at 1 atm and P_{do} is between 1 and 26 atm.

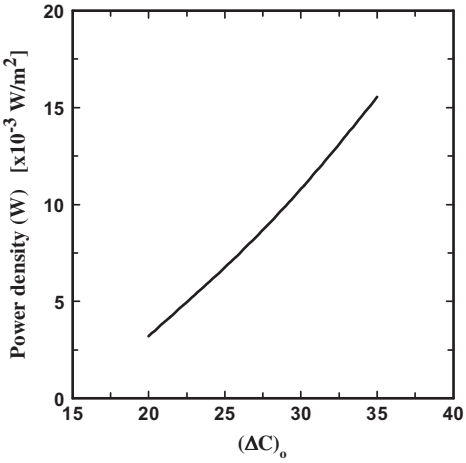

Fig. 8. Power density vs. ΔC_o (=($C_{do} - C_{fo}$)). Here, C_{do} is fixed at 35 g/l and C_{fo} is between 0 and 15 g/l.

The power density of our system was calculated at different inlet pressures of draw-fluid while fixing the pressure of feed-fluid at 1 atm. As in Eq. (13), power density is obtained by multiplying the water flux (J_w) and the pressure difference (ΔP) [2]. So, for comparison, the water flux and the power density, estimated for the different inlet pressure differences (ΔP_o), are shown in Fig. 7(a) and (b). The water flux (J_w) decreases with the increasing difference between inlet pressures (ΔP_o) of draw- and feed-fluids as shown in Figs. 3(a) and 7(a). So, when ΔP_o increases, the power density becomes a multiplication of the increasing ΔP_o and the decreasing J_w. Hence, as ΔP_o increases, the power density increases at first because of the increasing ΔP_o and then decreases later because of the decreasing J_w as shown in Fig. 7(b). In other words, the power density increases at first and decreases. The power density has a maximum value when ΔP_o is ($\Delta\pi/2$) in our system.

In the PRO system, the power generation is affected by the three limiting phenomena—ECP, ICP, and reverse water flux [14]. In general, increasing ΔC_o between feed- and draw-fluids increases the osmotic pressure, $\Delta\pi$ [15]. The osmotic pressure difference across the membrane drives the permeation of water from the dilute feed-fluid into the more concentrated draw-fluid. So the concentration difference affects the water flux and power. Power density is directly proportional to the difference of concentrations as shown in Fig. 8.

4. Conclusions

Mathematical modeling of the PRO system with the spiral wound module was carried out. The water flux (J_w) and the solute flux (J_s) across membrane were calculated. In addition, changes of concentration, flow rate, and pressure of channel-fluids were obtained. The followings were observed.

J_w decreases about 10% along the direction of draw-fluid in our system and increases slightly along the direction of feed-fluid. J_w becomes bigger when the inlet pressures difference between feed- and draw-fluids (ΔP_o) gets smaller. On the other hand, both J_w and J_s across membrane become bigger when the difference between the inlet concentrations (ΔC_o) of feed- and draw-fluids gets bigger.

The concentration of draw-fluid (C_d) decreases along the direction of draw-fluid. However, the concentration of feed-fluid (C_f) increases along the direction of feed-fluid. As ΔC_o becomes large, the flow rate of draw-fluid (F_d) increases and that of the feed fluid (F_f) decreases. On the other hand, as ΔP_o becomes large, F_d decreases and F_f increases.

Power density is directly proportional to ΔC_o. In addition, power density increases at first and decreases later with the increasing ΔP_o.

Acknowledgments

This work was supported by the New & Renewable Energy Technology Development Program of the Korea Institute of Energy Technology Evaluation and Planning (KETEP) grant funded by the Korea government Ministry of Knowledge Economy (No. 20103020070060). This work was also supported by 2013 Hongik University Research Fund.

Symbols

A	—	solvent (i.e. water) permeability coefficient, m/(atm s)
B	—	solute (i.e. salt) permeability coefficient, m/s
b	—	friction parameter in the channel, atm s/m^4
C_d, C	—	concentration of salt in the channel, g/l
c_d, c_f	—	dimensionless concentration of salt in the channel
D	—	diffusion coefficient in the porous support layer (=$D_m\varepsilon/\tau$), m^2/s
F_d, F_f	—	volumetric flow rate in the channel, m^3/s
J_w	—	water flux, m/s
J_s	—	solute flux, mol/m^{2}s
k	—	mass transfer coefficient of solute, m/s
P_d, P_f	—	pressure in the channel, atm
L	—	x-directional length in the feed channel, m
R	—	gas constant (=0.082), atm m^3/(mol K)
$S(=t_s\tau/\varepsilon)$	—	structure parameter of the support layer, m
t_f, t_d	—	height of the channel, m
t_s	—	thickness of the support layer, m
T	—	temperature, K
v_f, v_d	—	velocity of fluid in the channel, m/s
W	—	power density, W/m^2

w — y-directional width in the draw channel, m
X — dimensionless x-directional distance along the flow in the draw channel
x — x-directional distance along the flow in the draw channel, m
Y — dimensionless y-directional distance along the flow in the feed channel
y — y-directional distance along the flow in the feed channel, m

Greek

ε — porosity of the support layer
τ — tortuosity of pores in the support layer

Subscripts

d — draw channel
f — feed channel
o — inlet condition
s — solute, i.e. salt
w — solvent, i.e. water

References

[1] A.T. Jones, W. Rowley, Global perspective: Economic forecast for renewable ocean energy technology, Mar. Technol. Soc. J. 36 (2003) 85–90.
[2] N.Y. Yip, A. Tiraferri, W.A. Phillip, J.D. Schiffman, L.A. Hoover, Y.C. Kim, M. Elimelech, Thin-film composite pressure retarded osmosis membranes for sustainable power generation from salinity gradients, Environ. Sci. Technol. 45 (2011) 4360–4369.
[3] K.S. Kim, W. Ryoo, M.S. Chun, G.Y. Chung, S.O. Lee, Transport analysis in reverse electrodialysis with pulsatile flows for enhanced power generation, Korean J. Chem. Eng. 29 (2012) 162–168.
[4] K. Gerstandt, K.V. Peinemann, S.E. Skilhagen, T. Thorsen, T. Holt, Membrane processes in energy supply for an osmotic power plant, Desalination 224 (2008) 64–70.
[5] W.A. Phillip, J.S. Yong, M. Elimelech, Reverse draw solute permeation in forward osmosis: Modeling and experiments, Environ. Sci. Technol. 44 (2010) 5170–5176.
[6] A. Achilli, T.Y. Cath, A.E. Childress, Power generation with pressure retarded osmosis: An experimental and theoretical investigation, J. Membr. Sci. 343(1–2) (2009) 42–52.
[7] S. Sundaramoorthy, G. Srinivasan, D.V.R. Murthy, An analytical model for spiral wound reverse osmosis membrane modules: Part I—Model development and parameter estimation, Desalination 280 (2011) 403–411.
[8] J. Schwinge, P.R. Neal, D.E. Wiley, D.F. Fletcher, A.G. Fane, Spiral wound modules and spacers: Review and analysis, J. Membr. Sci. 242 (2004) 129–153.
[9] S.T. Hwang, Fundamentals of membrane transport, Korean J. Chem. Eng. 28 (2011) 1–15.
[10] J.R. McCutcheon, M. Elimelech, Modeling water flux in forward osmosis: Implications for improved membrane design, AIChE J. 53 (2007) 1736–1744.
[11] S. Kim, E.M.V. Hoek, Modeling concentration polarization in reverse osmosis processes, Desalination 186 (2005) 111–128.
[12] S. Sundaramoorthy, G. Srinivasan, D.V.R. Murthy, An analytical model for spiral wound reverse osmosis membrane modules: Part II—Experimental validation, Desalination 277 (2011) 257–264.
[13] N.Y. Yip, M. Elimelech, Thermodynamic and energy efficiency analysis of power generation from natural salinity gradients by pressure retarded osmosis, Environ. Sci. Technol. 46 (2011) 5230–5239.
[14] N.Y. Yip, M. Elimelech, Performance limiting effects in power generation from salinity gradients by pressure retarded osmosis, Environ. Sci. Technol. 45 (2011) 10273–10282.
[15] L.Y. Hung, S.J. Lue, J.H. You, Mass-transfer modeling of reverse-osmosis on 0.5–2% salty water, Desalination 265 (2011) 67–73.